Title

Anticancer Efficacy of KRASG12C Inhibitors Is Potentiated by PAK4 Inhibitor KPT9274 in Preclinical Models of KRASG12C-Mutant Pancreatic and Lung Cancers.

Journal

Molecular Cancer Therapeutics, 22(12)

Authors

Khan, Husain
Aboukameel, Amro
Alkhalili, Osama
et al.

Publication Date

2023-12-01

DOI

10.1158/1535-7163.MCT-23-0251

Anticancer Efficacy of KRAS^{G12C} Inhibitors Is Potentiated by PAK4 Inhibitor KPT9274 in Preclinical Models of *KRAS*^{G12C}-Mutant Pancreatic and Lung Cancers

Husain Yar Khan[1], Misako Nagasaka[2,3], Amro Aboukameel[1], Osama Alkhalili[1], Md. Hafiz Uddin[1], Sahar F. Bannoura[1], Yousef Mzannar[1], Ibrahim Azar[1], Eliza W. Beal[1], Miguel E. Tobon[1], Steve H. Kim[1], Rafic Beydoun[1], Erkan Baloglu[4], William Senapedis[4], Bassel F. El-Rayes[5], Philip A. Philip[6,7], Ramzi M. Mohammad[1], Anthony F. Shields[1], Mohammed Najeeb Al Hallak[1], and Asfar S. Azmi[1]

ABSTRACT

KRAS^{G12C} inhibitors, such as sotorasib and adagrasib, have revolutionized cancer treatment for patients with *KRAS*^{G12C}-mutant tumors. However, patients receiving these agents as monotherapy often develop drug resistance. To address this issue, we evaluated the combination of the PAK4 inhibitor KPT9274 and KRAS^{G12C} inhibitors in preclinical models of pancreatic ductal adenocarcinoma (PDAC) and non–small cell lung cancer (NSCLC). PAK4 is a hub molecule that links several major signaling pathways and is known for its tumorigenic role in mutant Ras–driven cancers. We found that cancer cells resistant to KRAS^{G12C} inhibitor were sensitive to KPT9274-induced growth inhibition. Furthermore, KPT9274 synergized with sotorasib and adagrasib to inhibit the growth of *KRAS*^{G12C}-mutant cancer cells and reduce their clonogenic potential. Mechanistically, this combination suppressed cell growth signaling and downregulated cell-cycle markers. In a PDAC cell line–derived xenograft (CDX) model, the combination of a suboptimal dose of KPT9274 with sotorasib significantly reduced the tumor burden ($P = 0.002$). Similarly, potent antitumor efficacy was observed in an NSCLC CDX model, in which KPT9274, given as maintenance therapy, prevented tumor relapse following the discontinuation of sotorasib treatment ($P = 0.0001$). Moreover, the combination of KPT9274 and sotorasib enhances survival. In conclusion, this is the first study to demonstrate that KRAS^{G12C} inhibitors can synergize with the PAK4 inhibitor KPT9274 and combining KRAS^{G12C} inhibitors with KPT9274 can lead to remarkably enhanced antitumor activity and survival benefits, providing a novel combination therapy for patients with cancer who do not respond or develop resistance to KRAS^{G12C} inhibitor treatment.

Introduction

KRAS is one of the most common oncogenes in human cancers, with a particularly high mutation rate in pancreatic, colorectal, and lung cancers (1). Given its high prevalence in various malignancies, extensive efforts have been dedicated to exploring the potential for the direct inhibition of mutated KRAS. A number of small-molecule inhibitors, including sotorasib (AMG510) and adagrasib (MRTX849), have been developed that target the *KRAS*^{G12C}-mutant protein in cancer cells (2, 3). These inhibitors rely on the mutant cysteine to bind irreversibly to the switch II pocket of the GDP-bound KRAS protein, resulting in the trapping of KRAS in the inactive state and the inhibition of KRAS-dependent signaling (4).

Clinical trials are currently underway to assess the effects of these covalent inhibitors of KRAS^{G12C} on patients with cancer. Preliminary trials of sotorasib and adagrasib have reported encouraging results (5, 6). The emergence of these new covalent inhibitors has presented an unparalleled opportunity to target critical *KRAS* mutations. Notably, in 2021, the FDA granted accelerated approval of sotorasib for treating patients with *KRAS*^{G12C}-mutated locally advanced or metastatic non–small cell lung cancer (NSCLC; ref. 7). Recently, adagrasib has become the second KRAS inhibitor to receive FDA approval (8).

While studies on KRAS^{G12C} inhibitors (KRAS^{G12Ci}) have demonstrated encouraging outcomes, the fact that some patients do not respond to these therapies, show limited durable response, and experience recurrence suggests that the issue of intrinsic or acquired resistance is an inevitable challenge for such molecular targeted therapies. This resistance is likely due to the activation of an alternative pathway or the selection of minor drug-resistant mutants. Therefore, circumventing drug resistance by developing novel combination therapies that can maximize the therapeutic potential of these KRAS^{G12C} drugs is the need of the hour.

A relatively less explored effector of RAS oncogenic signaling is PAK4, which belongs to a group of serine/threonine kinases called p21-activated kinases (PAK). PAK4 has emerged as an appealing target for cancer therapy due to its strategic role as a hub molecule linking major signaling pathways, including the KRAS–MAPK pathway (9, 10). PAK4 is often upregulated in various types of cancer, including NSCLC, prostate, gastric, and breast cancers (11–14). In cancers such as pancreatic, ovarian, and oral squamous cell carcinoma, amplification of the *PAK4* gene is frequently observed (15–17). PAK4 plays a critical role in controlling cell proliferation, survival, invasion, metastasis, epithelial–mesenchymal transition, and drug resistance

[1]Department of Oncology, Barbara Ann Karmanos Cancer Institute, Wayne State University School of Medicine, Detroit, Michigan. [2]University of California Irvine School of Medicine, Orange, California; Chao Family Comprehensive Cancer Center, Orange, California. [3]Division of Neurology, Department of Internal Medicine, St. Marianna University, Kawasaki, Japan. [4]Karyopharm Therapeutics, Newton, Massachusetts. [5]University of Alabama, Birmingham, Alabama. [6]Henry Ford Health, Detroit, Michigan. [7]Department of Pharmacology, Wayne State University, Detroit, Michigan.

Corresponding Author: Asfar Sohail Azmi, Department of Oncology, Wayne State University School of Medicine, 4100 John R, Detroit MI 48201. E-mail: azmia@karmanos.org

Mol Cancer Ther 2023;22:1422–33

doi: 10.1158/1535-7163.MCT-23-0251

both *in vitro* and *in vivo*, ultimately contributing to cancer progression (10–12, 18–20). It is noteworthy that PAK4, as opposed to other PAK isoforms, can transform normal cells (19). A recent study demonstrated that PAKs were activated in KRAS^{G12Ci}-resistant cancer cells and PAKs mediate this resistance through the activation of MAPK and PI3K pathways (21). PAK4 signaling has also been reported to play a critical role in resistance to chemotherapy in gastric and cervical cancers (22, 23). Moreover, targeting PAK4 has been shown to inhibit Ras-mediated oncogenic signaling (24).

KPT9274, a small-molecule inhibitor that targets PAK4, has been studied as a potential cancer therapy in preclinical and early-stage clinical trials (20). In this study, we report for the first time that KRAS^{G12Ci}-resistant cancer cells are sensitive to KPT9274, providing a rationale for testing PAK4 inhibitors (PAK4i) in combination with KRAS^{G12C} inhibitors as an effective combination therapy. Using *KRAS*^{G12C}-mutant preclinical cancer models, we demonstrate that KPT9274 synergizes with *KRAS*^{G12C} inhibitors and enhances their anticancer activity when used in combination as well as in maintenance.

Materials and Methods

Cell lines, drugs, and reagents

MIA PaCa-2, NCI-H358 and HPAC cells were purchased from the ATCC in 2012, 2021, and 2022, respectively. NCI "Rasless" mouse embryonic fibroblast (MEF) cell lines (KRAS 4B G12C and KRAS 4B G12D) were obtained from the NCI (Rockville, MD) in 2019. MIA PaCa-2, HPAC, and MEF cell lines were maintained in DMEM (Thermo Fisher Scientific), while NCI-H358 was maintained in RPMI1640 (Thermo Fisher Scientific), supplemented with 10% FBS, 100 U/mL penicillin, and 100 μg/mL streptomycin in a 5% CO_2 atmosphere at 37°C. All experiments were performed within 20 passages of the cell lines. The cell lines have been tested and authenticated in a core facility of the Applied Genomics Technology Center at Wayne State University (Detroit, MI). The method used for testing was short tandem repeat (STR) profiling using the PowerPlex 16 System (Promega). *Mycoplasma* testing was routinely performed on the cell lines using PCR. AMG510 (25) and MRTX849 (26) were procured from Selleck Chemical LLC and KPT9274 (27) provided by Karyopharm Therapeutics were dissolved in DMSO to make 10 mmol/L stock solutions. KPT9274 is example 728 in patent US20160368904A1 (27) and its chemical structure is given in Supplementary Fig. S1. The drug control used for *in vitro* inhibitor experiments was cell culture medium containing 0.1% DMSO.

Cell viability assay and synergy analysis

Cells were seeded in 96-well culture plates at a density of 3×10^3 cells per well. The growth medium was removed after overnight incubation and replaced with 100 μL of fresh medium containing the drug at various concentrations serially diluted from stock solution using an OT-2 liquid handling robot (Opentrons). After 72-hour exposure to the drug, MTT (3-(4,5-dimethylthiazol-2-yl)-2,5-diphenyltetrazolium bromide) assay was performed according to the procedure described previously (28). Using the cell proliferation data (six replicates for each dose), IC_{50} values were calculated using the GraphPad Prism 4 software.

For the synergy analysis, cells were treated with three different concentrations of either MRTX849/AMG510, KPT9274, or a combination of KPT9274 with MRTX849/AMG510 at the corresponding doses for 72 hours (six replicates for each treatment). The drug concentration ratio was kept constant across all the three dose combinations tested. Cell growth index was determined using MTT assay. The resulting cell growth data were used to calculate the combination index (CI) using the CalcuSyn software (Biosoft).

Colony formation assay

MIA PaCa-2, HPAC, and MIA-AMG-R cells were seeded at a density of 500 cells per well in 6-well plates and exposed to single-agent or combination drug treatments for 72 hours. At the end of the treatment, the drug-containing medium was removed and replaced with fresh medium. The plates were incubated in a CO_2 incubator for an additional 10 days (for MIA PaCa-2 colonies) or 1 week (for HPAC and MIA-AMG-R colonies). After the incubation was over, the medium was removed from the wells and the colonies were fixed with methanol and stained with crystal violet for 15 minutes. The plates were washed and dried, and the colonies were photographed.

Spheroid formation and disintegration assays

MIA PaCa-2 and NCI-H358 cells were trypsinized, collected as single-cell suspensions using cell strainer, and resuspended in 3D Tumorsphere Medium XF (PromoCell). For the tumor formation assay, 1,000 cells were plated in each well of an ultra-low attachment 6-well plate (Corning) and treated with KPT9274, MRTX849, or a combination of KPT9274 and MRTX849 twice a week for 1 week. For the spheroid disintegration assay, 200 cells were plated in each well of an ultra-low attachment round-bottom plate (Corning). The medium was replenished every three days and spheroid growth was monitored. Once sizable spheroids were formed, they were subjected to treatment with drugs for three days. At the end of the treatment, spheroids were photographed under an inverted microscope.

RNA isolation and mRNA real-time RT-qPCR

Total RNA from cancer cell lines or mouse tumors was extracted and purified using the RNeasy Mini Kit and RNase-free DNase Set (QIAGEN) following the protocol provided by the manufacturer. The expression levels of CDK4, CDK6, Cyclin D1, β-catenin and PAK4 mRNA were analyzed by real-time RT-qPCR using High-Capacity cDNA Reverse Transcription Kit and SYBR Green Master Mix from Applied Biosystems. The conditions and procedure for RT-qPCR have been described previously (28). The sequences of primers used are listed in Supplementary Table S1.

Preparation of total protein lysates and Western blot analysis

For total protein extraction, cancer cells or tumor tissues were lysed in RIPA buffer and protein concentrations were measured using the bicinchoninic acid (BCA) protein assay (PIERCE). A total of 40 μg of protein lysate from treated and untreated cells was resolved using 10% SDS-PAGE and transferred onto nitrocellulose membranes. The membranes were incubated with the following primary antibodies (Cell Signaling Technology) at 1:1000 dilution in 3% non-fat dry milk: anti-phopho-MEK (#9121), anti-MEK (#9122), anti-phospho-S6 (#2211), anti-S6 (#2217), anti-phospho-Erk $^1/_2$ (# 4370), anti-Erk $^1/_2$ (# 9102), anti-phospho-AKT (#9271), anti-AKT (#9272), anti-DUSP6 (# 50945), anti-CDK4 (# 12790), anti-CDK6 (# 13331), anti-cyclin D1 (# 55506). While anti-GAPDH (# sc-47724; Santa Cruz Biotechnology) was used at a dilution of 1:3,000. Incubation with either 1:2000 diluted HRP-linked secondary antibodies (# 7074/7076; Cell Signaling Technology) in 3% nonfat dry milk or 1:10,000 diluted IRDye 800CW goat anti-mouse/IRDye 680RD goat anti-rabbit secondary antibodies (#827–08364/926–68171; LI-COR Biosciences) in 3% BSA solution was subsequently performed at room temperature for 1 hour. The

signal was detected using the ECL chemiluminescence detection system (Thermo Fisher Scientific) and the ChemiDoc Imaging system (Bio-Rad) or the LI-COR Odyssey DLx Imager.

KRAS^{G12C}-mutant cell-derived tumor xenograft studies

In vivo studies were conducted under the Wayne State University's Institutional Animal Care and Use Committee (IACUC) approved protocol in accordance with approved guidelines. The experiments were approved by the institute's IACUC (#18–12–0887 for pancreatic ductal adenocarcinoma (PDAC) *in vivo* study and #22–01–4355 for NSCLC *in vivo* study).

PDAC (MIA PaCa-2) cell-derived tumor xenograft model

After adaptation in our animal housing facility, 4- to 5-week-old female ICR-SCID mice (Taconic Biosciences) were subcutaneously implanted with MIA PaCa-2 cells. A total of 1×10^6 cells suspended in 200 μL PBS were injected unilaterally into the left flank of donor mice using a BD 26Gx 5/8 1 mL Sub-Q syringe. Once the tumors reached about 5%–10% of the donor mice body weight, the donor mice were euthanized, tumors were harvested, and fragments were subsequently implanted into recipient mice. Seven days posttransplantation, the recipient mice were randomly divided into four groups of 6 mice each and received either vehicle, or KPT9274 (100 mg/kg every day $\times$ 5×3 weeks), or sotorasib (25 mg/kg every day $\times$ 5×3 weeks), or their combination by oral gavage. Tumor volumes were determined using the formula $0.5 \times L \times W^2$ in which L refers to length and W refers to width of each tumor. Upon completion of drug dosing, tumor tissue from the control or treatment groups were used for IHC and molecular analysis.

NSCLC (NCI-H358) cell-derived tumor xenograft model

NCI-H358 cells were washed in PBS and then suspended in cold PBS at a concentration of 100,000 cells per 100 μL. The cell suspensions were mixed with an equal volume of Cultrex extracellular matrix (ECM; Trevigen, #3432–005–01) and kept on ice. Female ICR-SCID mice, aged 4–5 weeks, were injected with a mixture of ECM and cells into the left flank of each mouse. For the efficacy study, the mice were randomized into four groups of 5 mice each. Mice were orally administered sotorasib (25 mg/kg every day $\times$ 5) for 15 days in the single agent and combination groups, while KPT9274 (150 mg/kg every day $\times$ 5) was dosed for 26 days in both groups. For the survival study, mice unilaterally transplanted with NCI-H358 cells were randomly divided into four treatment groups of 7 mice each. Sotorasib and KPT9274 were administered at the aforementioned doses for 3 and 5 weeks, respectively, by oral gavage.

Immunostaining

Paraffin sections of MIA PaCa-2–derived tumors were processed and stained with hematoxylin and eosin (H&E) and antibodies in the core facility at the Department of Oncology, Wayne State University/Karmanos Cancer Institute (Detroit, MI). The following antibodies were used for IHC staining: anti-Ki67 (catalog no. M7240; Dako), anti-KRAS (catalog no. 41–570–0; Thermo Fisher Scientific) and anti-PAK4 (catalog no. TA807297; Origene Technologies).

Statistical analysis

The Student t test was used to compare statistically significant differences between the groups. Wherever suitable, the experiments were performed at least three times. The data were also subjected to unpaired two-tailed Student t test wherever appropriate and $P < 0.05$ was considered statistically significant.

Data availability

The data generated in this study are available upon request from the corresponding author.

Results

KPT9274 induces growth inhibition in PDAC cells resistant to KRAS^{G12Ci}

KRAS^{G12Ci}-resistant cell lines were generated in our laboratory as described previously (29). To establish the durability of drug resistance, we compared the IC_{50} values of the sotorasib-resistant cell line (MIA-AMG-R) that we developed earlier with those of sotorasib-sensitive parental cell line (MIA PaCa-2). We observed more than 42-fold increase in the IC_{50} of sotorasib for the MIA-AMG-R cells, confirming that these cells maintained their resistance to sotorasib even in the absence of sotorasib from their growth medium (**Fig. 1A**). Subsequently, this drug-resistant cell line was treated with KPT9274 and found to be sensitive to KPT9274-induced inhibition of cell growth (**Fig. 1B**). This establishes that KRAS^{G12Ci}-resistant cancer cells can potentially respond to the PAK4i KPT9274.

Next, we used Synthetic Lethal analysis via Network topology (SLant) to predict human synthetic lethal (SSL) interactions (30). This approach identifies and leverages conserved patterns in the topology of protein interaction networks for its predictions. Using this approach, we obtained experimentally validated synthetic lethal interactions of PAK4 from the Slorth database (http://slorth.biochem.sussex.ac.uk/welcome/index) and found the interaction of PAK4 with KRAS to be synthetic lethal (Supplementary Fig. S2).

Combining KPT9274 with KRAS^{G12C} inhibitors synergistically suppresses the proliferation of *KRAS*^{G12C}-mutant cells

KRAS^{G12C}-mutant MIA PaCa-2 (PDAC) and NCI-H358 (NSCLC) cells were exposed to MRTX849/AMG510 and KPT9274 at different dose combinations. As shown in **Fig. 2A** and **B**, all three dose combinations tested demonstrated synergistic inhibition of MIA PaCa-2 cell proliferation (CI < 1). Similar synergistic effects (CI < 1) in suppressing cell growth were also observed with the NCI-H358 cells treated with different dose combinations of the two drugs (**Fig. 2C** and **D**). Likewise, the combination of KRAS^{G12C} inhibitors with KPT9274 exerted synergistic growth-inhibitory effects on another *KRAS*^{G12C}-mutant NSCLC cell line NCI-H2122 (Supplementary Fig. S3). Furthermore, the combination doses of KPT9274 with KRAS^{G12C} inhibitors proved ineffective in a *KRAS*^{G12D}-mutant PDAC cell line HPAC, indicating their specificity for *KRAS*^{G12C}-mutant models (Supplementary Fig. S4A and S4B). Moreover, the AMG510-resistant MIA PaCa-2 cell line (MIA-AMG-R) also did not respond to treatment with either MRTX849 or AMG510 but showed sensitivity toward KPT9274-induced growth inhibition (Supplementary Fig. S4C and S4D).

This drug combination was also tested on NCI "Rasless" MEFs carrying *KRAS*^{G12C} or *KRAS*^{G12D} mutations. KPT9274 synergized with MRTX849 at all dose combinations yielding suppressed growth of *KRAS*^{G12C}-mutant MEFs (Supplementary Fig. S5A). As expected, the *KRAS*^{G12D} MEFs (KRAS4B G12D) were refractory to any such growth inhibition (Supplementary Fig. S5B).

Combination of KPT9274 with KRAS^{G12Ci} reduces the clonogenic potential and effectively disrupts spheroids

The combinations of KPT9274 with MRTX849 were evaluated for their effects on the colony-forming ability of MIA PaCa-2 cells.

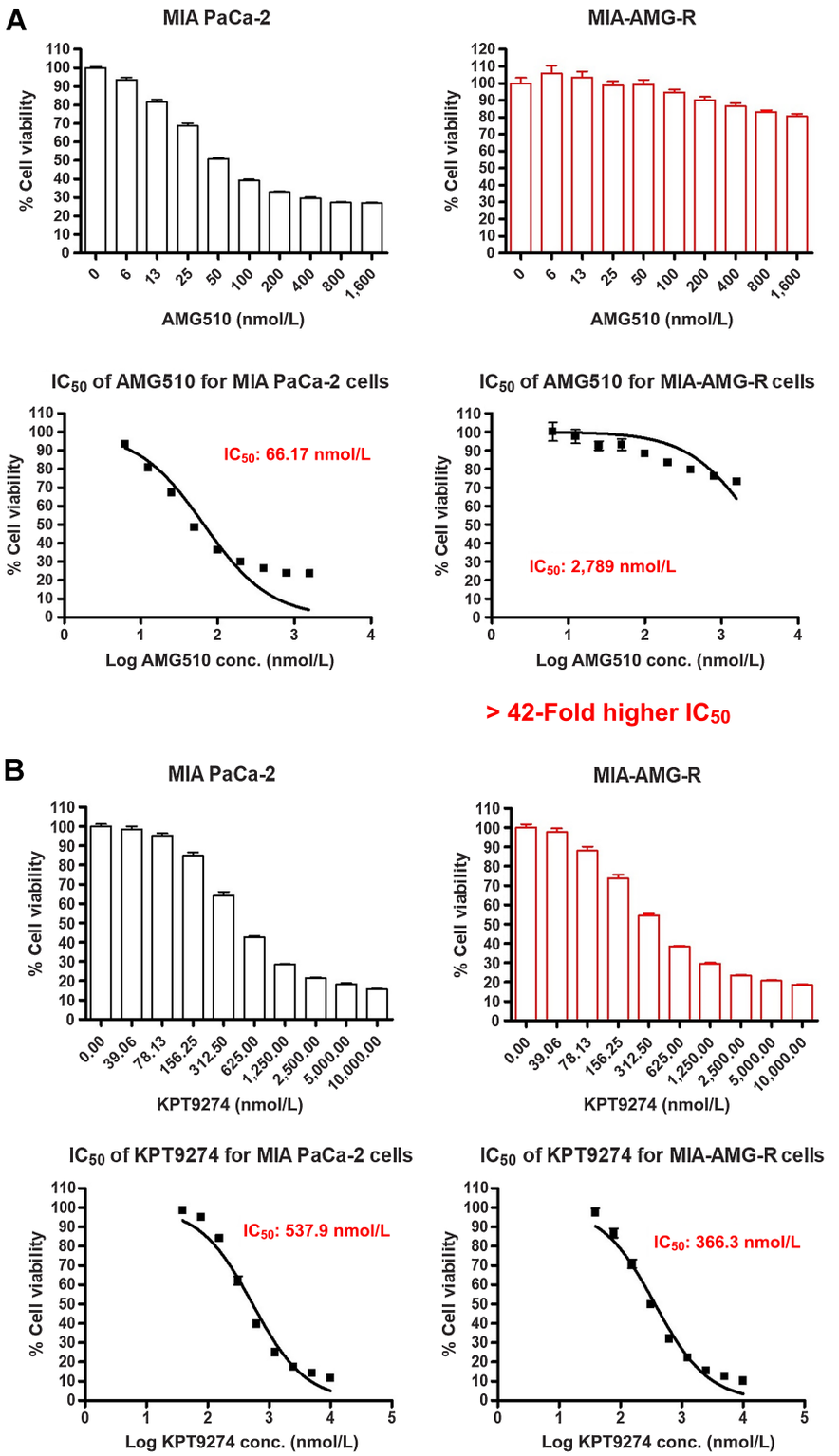

Figure 1.

KPT9274 induces growth inhibition in KRAS^{G12Ci}-resistant cancer cells. **A,** *KRAS*^{G12C}-mutant MIA PaCa-2 cells exposed to incremental doses of AMG510 in long-term cell culture eventually developed drug resistance (MIA-AMG-R) as shown by their unresponsiveness to drug treatment in MTT assay and > 42-fold increase in the drug IC_{50} value compared with parental MIA PaCa-2 cells. **B,** AMG510-resistant MIA PaCa-2 cell line (MIA-AMG-R) show sensitivity toward KPT9274-induced growth inhibition. Parental as well as resistant cells were treated with KPT9274 for 72 hours and MTT assay was performed as described in Materials and Methods. All results are expressed as percentage of control ± SEM of six replicates.

The results of a clonogenic assay clearly demonstrated that the combination treatments of KPT9274 with the KRAS^{G12Ci} resulted in a decrease in colony numbers as well as the size of colonies formed by MIA PaCa-2 cells (**Fig. 3A**). In similar clonogenic assays, *KRAS*^{G12D}-mutant HPAC cells and sotorasib-resistant MIA-AMG-R cells showed no response to treatment with MRTX849. However, KPT9274 was able to induce suppression of colony formation by these cells (**Fig. 3A**; Supplementary Fig. S6). These findings further underscore the efficacy

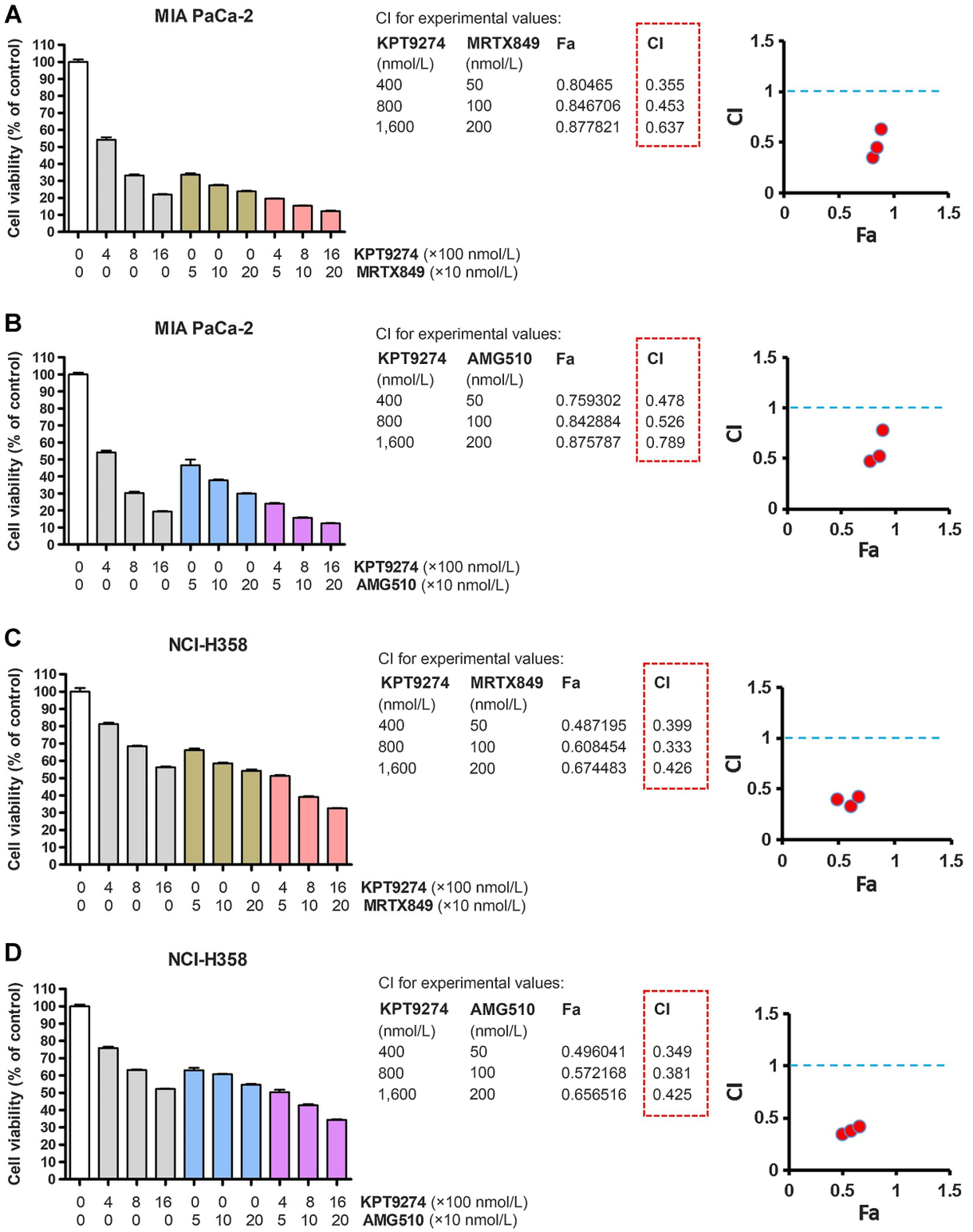

Figure 2.

KPT9274 and *KRAS*^{G12C} inhibitors show synergistic effects on the inhibition of cell proliferation *in vitro*. Different dose combinations of KPT9274 with MRTX849 (**A** and **C**) and AMG510 (**B** and **D**) synergistically inhibit the proliferation of *KRAS*^{G12C}-mutant PDAC cell line MIA PaCa-2 and NSCLC cell line NCI-H358, as indicated by combination index (CI) values less than 1. Cell viability was determined by MTT assay and synergy analysis was performed by using CalcuSyn software. All results are expressed as percentage of control ± SEM of six replicates.

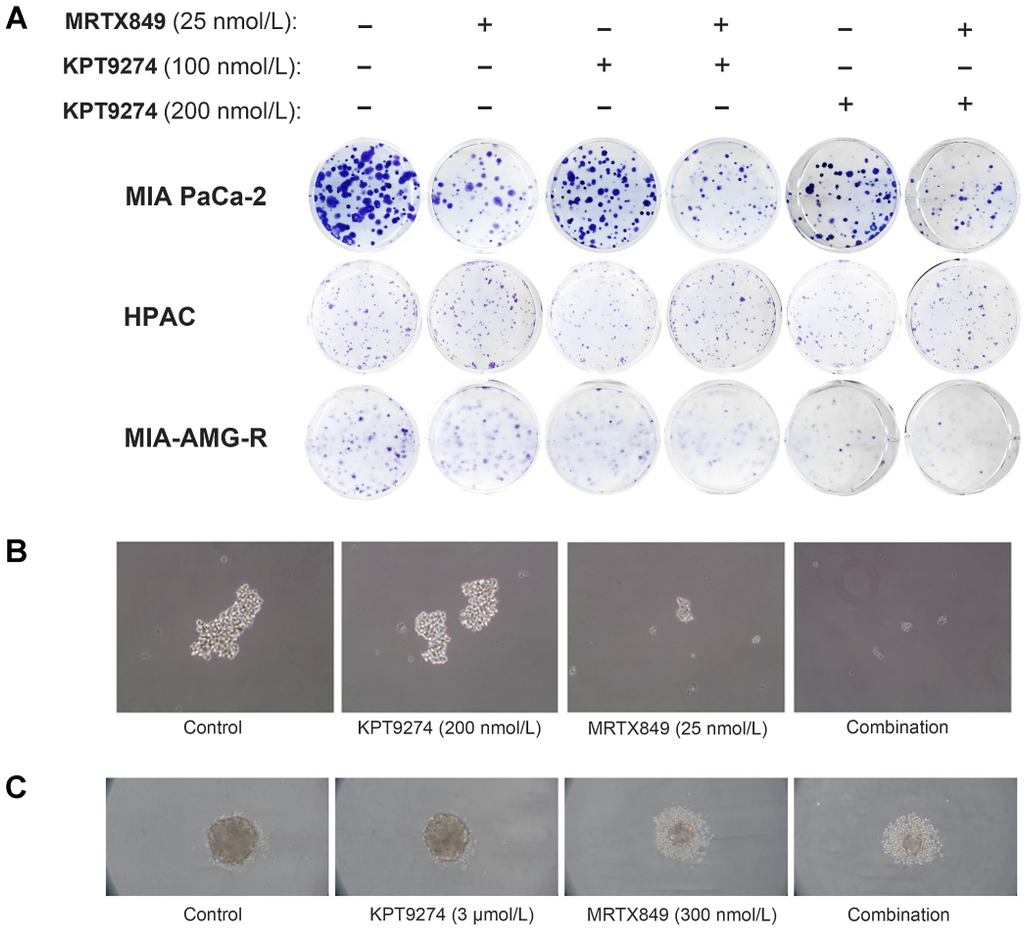

Figure 3.

KPT9274 and KRAS^{G12Ci} combination reduces the clonogenic potential, prevents spheroid formation, and induces spheroid disintegration. **A,** Combination of KPT9274 with MRTX849 inhibits the ability of *KRAS*^{G12C}-mutant MIA PaCa-2 cells to form colonies. *KRAS*^{G12D}-mutant HPAC cells and sotorasib-resistant MIA-AMG-R cells show no susceptibility to treatment with MRTX849. Cells seeded in 6-well plates (500 cells/well) were treated with indicated doses of the drugs for 72 hours and the colonies were fixed and stained after 10 days (MIA PaCa-2) or 1 week (HPAC and MIA-AMG-R). KPT9274 and MRTX849 combination treatment (**B**) suppresses spheroid formation in 3D cultures of MIA PaCa-2 cells and (**C**) enhances disintegration of spheroids formed by NCI-H358 cells. For spheroid formation assay, 1,000 MIA PaCa-2 cells in tumorsphere media were seeded in each well of ultra-low attachment 6-well plates and treated the next day. For spheroid disintegration assay, 200 NCI-H358 cells in tumorsphere media were seeded in each well of ultra-low attachment plate and allowed to form spheroids before being subjected to drug treatment. Images are representative of three replicates.

of this combination approach for targeting *KRAS*^{G12C}-mutant cancer cells *in vitro*.

The sensitivity of cells in 3D culture is believed to provide a more accurate prediction of *in vivo* efficacy because it is highly correlated with drug response in xenograft models (31). Previously, we have shown that PAK4i can target PDAC cancer stem cells (20). Therefore, we performed a spheroid formation assay, in which treatment of MIA PaCa-2 cells in a 3D culture medium with a combination of KPT9274 with MRTX849 prevented the formation of spheroids (**Fig. 3B**). We further tested this combination in a spheroid disintegration assay, in which *KRAS*^{G12C}-mutant NCI-H358 cells were first allowed to grow into sizable spheroids in a 3D culture medium and then exposed to the drugs for three days. The combination treatment resulted in enhanced disintegration of the spheroids (**Fig. 3C**; Supplementary Fig. S7). These results demonstrate the efficacy of PAK4i and KRAS^{G12Ci} combination in 3D cell growth models of *KRAS*^{G12C}-mutant PDAC and NSCLC.

KPT9274 and *KRAS*^{G12Ci} combination prevents cell-cycle progression and suppresses cell growth signaling

Transcriptional expression of cell-cycle markers CDK4, CDK6, and cyclin D1 were found to be reduced in NCI-H358 cells as a result of treatment with KRAS^{G12Ci} AMG510 or its combination with KPT9274 (**Fig. 4A–C**). Furthermore, we observed that the combination treatment reduced the levels of β-catenin. which is an important cytoplasmic protein that plays a key role in the Wnt signaling pathway and is also a direct effector of PAK4 (**Fig. 4D**). Crosstalk between the Wnt/β-catenin and RAS-ERK pathways and its role in tumorigenesis is already known (32).

The combination of KPT9274 and MRTX849 was able to sustain the inhibition of the ERK signaling pathway induced by the KRAS^{G12Ci} MRTX849 in MIA PaCa-2 cells as indicated by the downregulation of MEK and ERK phosphorylation (**Fig. 4E** and **F**). This effect on the direct inhibition of KRAS activated ERK signaling contributes to the

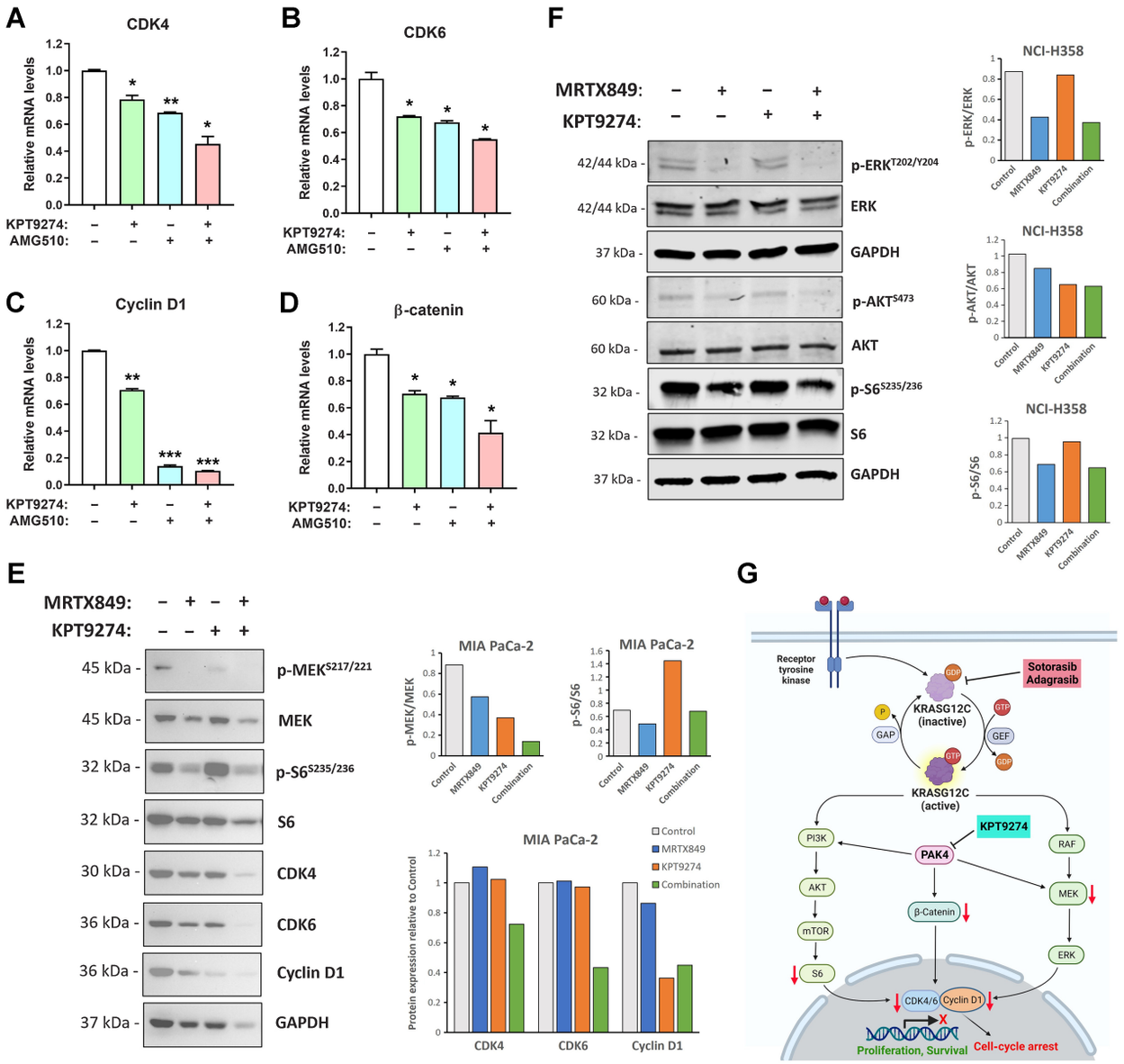

Figure 4.

KRAS^{G12C} inhibitors in combination with KPT9274 prevent cell-cycle progression and inhibit cell growth signaling. Relative mRNA levels of CDK4 (**A**), CDK6 (**B**), Cyclin D1 (**C**), and β-catenin (**D**) in NCI-H358 cells treated with either KPT9274 (500 nmol/L), AMG510 (50 nmol/L) or their combination for 24 hours. **E,** Immunoblots showing suppression of MEK phosphorylation, MEK expression, S6 phosphorylation, S6 ribosomal protein expression, as well as inhibition of CDK4, CDK6 and cyclin D1 protein expression in MIA PaCa-2 cells treated with a combination of MRTX849 (25 nmol/L) and KPT9274 (100 nmol/L) for 24 hours. **F,** Immunoblots showing suppression of ERK phosphorylation, AKT phosphorylation, and S6 phosphorylation in NCI-H358 cells treated with a combination of MRTX849 (50 nmol/L) and KPT9274 (500 nmol/L) for 6 hours. The quantitative analysis of mean pixel density of the blots was performed using NIH ImageJ 1.5Oi software. **G,** Schematic of the proposed mechanisms by which the combination of *KRAS*^{G12Ci} and KPT9274 induces antineoplastic activity. This drug combination can block multiple nodes (represented with red arrows) of the cell proliferation and survival machinery. Created with BioRender.com (License#*VA259JMADX*).

suppression of cancer cell proliferation. Furthermore, the combination also downregulated S6 expression in MIA PaCa-2 cells (**Fig. 4E**), while reducing S6 and AKT phosphorylation in NCI-H358 cells (**Fig. 4F**). Mitogens and growth factors induce the phosphorylation of S6 ribosomal protein, which is downstream of the PI3K/Akt cell survival pathway. Phosphorylation of S6 ribosomal protein correlates with an increase in translation of mRNA transcripts that encode proteins involved in cell-cycle progression, as well as ribosomal proteins and elongation factors required for translation (33). Hence, the downregulation of S6 and AKT phosphorylation by the combination of PAK4i and KRAS^{G12Ci} can result in the suppression of cancer cell growth. Moreover, MRTX849 in combination with KPT9274 remarkably reduced the protein expression of the cell-cycle markers CDK4, CDK6 and cyclin D1 in MIA PaCa-2 cells (**Fig. 4E**).

Evidently, the combinations of KPT9274 and KRAS^{G12C} inhibitors induced cell-cycle arrest in *KRAS*^{G12C}-mutant cancer cells by downregulating cyclin D1 and CDK4/6 expression which prevented cell-cycle progression from G_1 to S-phase. This may be another mechanism by which this novel combination can mediate its anticancer effects. On the basis of the molecular evidence obtained in this study, we have presented a schema of the possible mechanisms through which KRAS^{G12C} inhibitor(s) and KPT9274 combination can exert its effects on *KRAS*^{G12C}-mutant cancer cells (**Fig. 4F**).

Sotorasib and KPT9274 combination is more efficacious than single-agent sotorasib in a *KRAS*^{G12C}-mutant PDAC *in vivo* model

To assess the *in vivo* effect of sotorasib either as a single agent or in combination with KPT9274, a MIA PaCa-2 subcutaneous tumor xenograft model was established in ICR-SCID mice. The tumor-bearing mice were orally treated with suboptimal doses of either KPT9274 (100 mg/kg every day × 5 × 3 weeks), or sotorasib at one-fourth of MTD (25 mg/kg every day × 5 × 3 weeks) or a combination of sotorasib (25 mg/kg every day × 5×3 weeks) and KPT9274 (100 mg/kg every day × 5 × 3 weeks). Oral administration of the combination led to significant reduction in tumor volumes (**Fig. 5A**), tumor weights (**Fig. 5B**), and tumor sizes (**Fig. 5C**) as compared with single-agent treatments. The drug treatments, either single agents or combination, caused no significant change in the body weights of mice during the course of the treatment (**Fig. 5D**). Also, we did not find any signs of organ toxicity or metastatic spread while performing gross animal autopsy.

Residual tumor profiling using IHC showed marked reduction in the proliferation marker Ki67, as well as inhibition of KRAS and PAK4 in the combination group (**Fig. 5E** and **F**). Interestingly, the PAK4i KPT9274 treatment resulted in reduced KRAS expression which suggests that PAK4 may also act upstream of KRAS, resulting in pronounced downregulation of KRAS signaling. In addition, Western blot analysis of the residual tumor tissue proteins revealed downregulation of ERK activation as a result of treatment with KPT9274, or sotorasib and more so with their combination (**Fig. 5G**). Expression of DUSP-6, a downstream target of ERK, was reduced in the tumor tissue from the combination group, as also the expression of cell cycle markers CDK4, CDK6, and cyclin D1, suggesting that the combination of PAK4i and KRAS^{G12Ci} induces cell-cycle arrest at the G_1 to S phase in the tumor cells, ultimately resulting in tumor growth inhibition (**Fig. 5H** and **I**). In addition, the expression levels of PAK4 mRNA were significantly decreased in the residual tumor from the combination group (**Fig. 5J**). These results, taken together, demonstrate the preclinical safety and efficacy of sotorasib and KPT9274 combination *in vivo*.

KPT9274 is effective as a maintenance therapy to sotorasib for durable tumor growth inhibition and enhances survival in a *KRAS*^{G12C}-mutant NSCLC *in vivo* model

To examine the effect of KPT9274 in preventing the relapse of tumors following the cessation of sotorasib treatment, we administered KPT9274, sotorasib, or their combination to mice harboring NCI-H358 tumor xenografts for 15 days, following which sotorasib treatment was withdrawn but treatment with KPT9274 was continued for an additional 11 days (**Fig. 6A**). Tumors relapsed in mice treated with single agent sotorasib a few days after treatment was stopped. However, mice receiving KPT9274 in combination with, and later as an adjunct to sotorasib therapy continued to show tumor remission. Significant reductions in tumor volumes, tumor weights, and tumor sizes were observed in the combination group compared with the single-agent groups at the end of the experiment (**Fig. 6B–D**). The response in the combination/maintenance arm of this *in vivo* study was durable and signifies not only the efficacy of KPT9274 in combination with KRAS^{G12Ci} but also highlights its utility as a maintenance therapy to prevent or delay tumor relapse.

The *KRAS*^{G12C}-mutant NSCLC NCI-H358 CDX model was also used to evaluate the effect of KPT9274 and sotorasib combination therapy on survival as an endpoint (**Fig. 6E**). The results demonstrate a remarkable enhancement in survival of mice that received a combination of KPT9274 (150 mg/kg every day × 5 × 5 weeks) and sotorasib (25 mg/kg every day × 5 × 3 weeks). Almost 29% (2/7) of the mice in the combination treatment group survived and remained tumor-free for as long as 150 days after NCI-H358 subcutaneous transplantation (**Fig. 6F**). This establishes that by incorporating KPT9274 as a combination partner in KRAS therapy, an increase in survival can be achieved.

Discussion

In this study, we show, for the first time, the synergistic anticancer effects of KRAS^{G12C} inhibitors and the PAK4i KPT9274. Our combination approach of cotargeting KRAS^{G12C} and PAK4 resulted in enhanced growth suppression of *KRAS*^{G12C}-mutant cells and cell-derived xenografts (CDX). This study brings forward a novel combination therapy for drug-resistant *KRAS*^{G12C}-mutant tumors and provide preclinical rationale for the use of KPT9274 in a clinical setting to prevent or delay the development of resistance in patients receiving KRAS^{G12Ci} monotherapy.

Targeting the KRAS oncoprotein has been a long-term objective in translational oncology. The development of inhibitors that can specifically target the KRAS^{G12C} protein has reignited hopes after decades of writing off KRAS as nontargetable. Following the initial success of sotorasib and adagrasib in clinical trials (5, 6), researchers in the field have doubled down on their efforts to target KRAS with renewed enthusiasm. The treatment options available to patients with the *KRAS*^{G12C} mutation have undoubtedly expanded with the FDA's recent approval of sotorasib and adagrasib (7, 8). Despite showing promise as potent targeted therapies, KRAS^{G12C} inhibitors as monotherapies have limited efficacy. Studies have shown that patients treated with these inhibitors develop drug resistance over time, highlighting the need for combination approaches that could potentially enhance the sensitivity of tumors to KRAS inhibitors when cotargeted.

There is a growing understanding of the importance of identifying synthetic lethality associated with KRAS and developing small-molecule inhibitors that target these synthetic lethal targets. Previously, we experimentally validated the synthetic-lethal interactions of KRAS^{G12C} inhibitors with nuclear export protein XPO1 inhibitor *in silico*, *in vitro* and *in vivo* (29). In this study, the identification of the existence of synthetic lethality between PAK4 and KRAS using the Slorth database rationalizes the significance of cotargeting PAK4 and KRAS.

PAK4 is activated through different signaling pathways in cancer and it also acts as a hub linking major oncogenic signaling pathways (9). Approximately 20% of patients with pancreatic cancer exhibit gene amplification of *PAK4*, and PAK4 kinase activity is enhanced in pancreatic tumors (34). In NSCLC, overexpression of *PAK4* is reportedly linked to metastasis, reduced survival rates, and an advanced stage of the disease (11). Knockdown of *PAK4* in *KRAS*-mutant colon cancer cells suppresses their proliferation and this

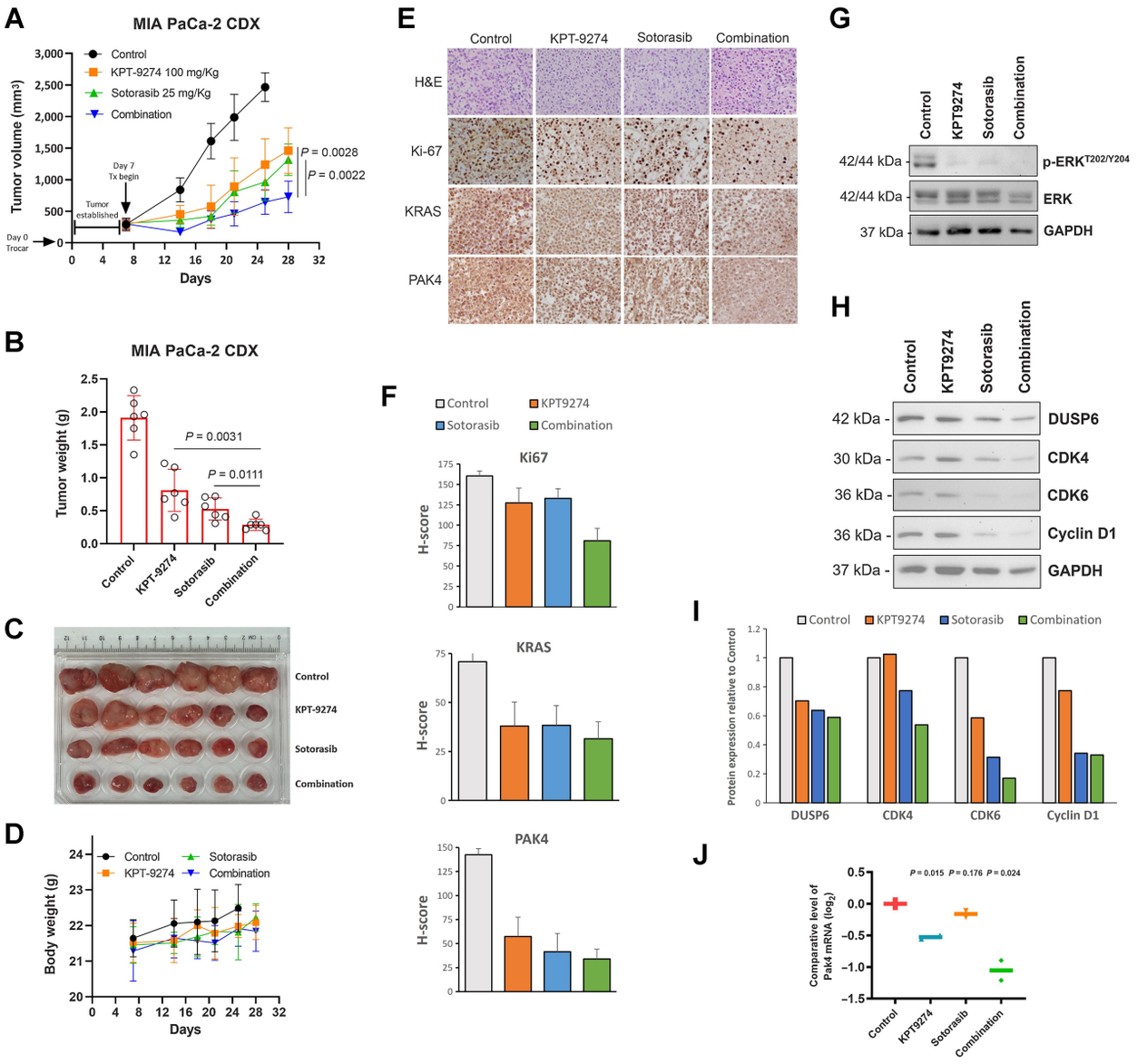

Figure 5.

Preclinical antitumor efficacy of KPT9274 and *KRAS*^{G12Ci} combination in a *KRAS*^{G12C}-mutant PDAC CDX model. Treatment of ICR-SCID mice carrying subcutaneous *KRAS*^{G12C}-mutant PDAC MIA PaCa-2 CDXs with a combination of KPT9274 and sotorasib resulted in significant reduction in tumor volumes (**A**), tumor weights (**B**), and tumor sizes (**C**). A two-tailed unequal variance Student *t* test was performed to statistically compare tumor volumes and tumor weights at the end of experiment. **D,** No substantial loss in the animal body weights was observed. **E,** IHC analysis showing (×400 magnification) reduction in Ki67, KRAS, and PAK4 in tumor tissues harvested from mice treated with the combination of KPT9274 and sotorasib. **F,** Quantitation of Ki67, KRAS, and PAK4 staining in three tumor tissue sections per group shown by H-score. **G** and **H,** Immunoblots showing downregulation of p-ERK, its downstream target DUSP6, and cell-cycle markers CDK4, CDK6, and cyclin D1 protein expression in the tumor tissue from the combination group. **I,** Quantitation of mean pixel density of the blots shown in H by ImageJ 1.5Oi software. **J,** The mRNA levels of PAK4 were also found to decrease in the combination group as determined by RT-qPCR.

suppression was independent of Raf/MEK/ERK or PI3K/AKT signaling, indicating that some unidentified PAK4 effectors were involved (10). While PAK4 mainly serves as a PI3K effector, it has also been reported to act as an upstream regulator of PI3K in driving resistance to cisplatin in gastric and cervical cancer cells (22, 23), suggesting the existence of a feedback loop between Ras/PI3K and PAK4. Very recently, ablation of Kras oncogene has been shown to induce massive tumor regression and prevent the emergence of sotorasib resistance (35). However, Kras-ablated pancreatic cancer cells have earlier been reported to exhibit PI3K-dependent MAPK signaling (36). Being an effector of PI3K, PAK4 can serve as a potential pharmacologic target, the inhibition of which can blunt the PI3K-dependent survival signaling and thereby augment the efficacy of KRAS therapies. On the basis of this accumulating body of evidence, PAK4 has been implicated as an attractive target in cancers driven by mutant KRAS.

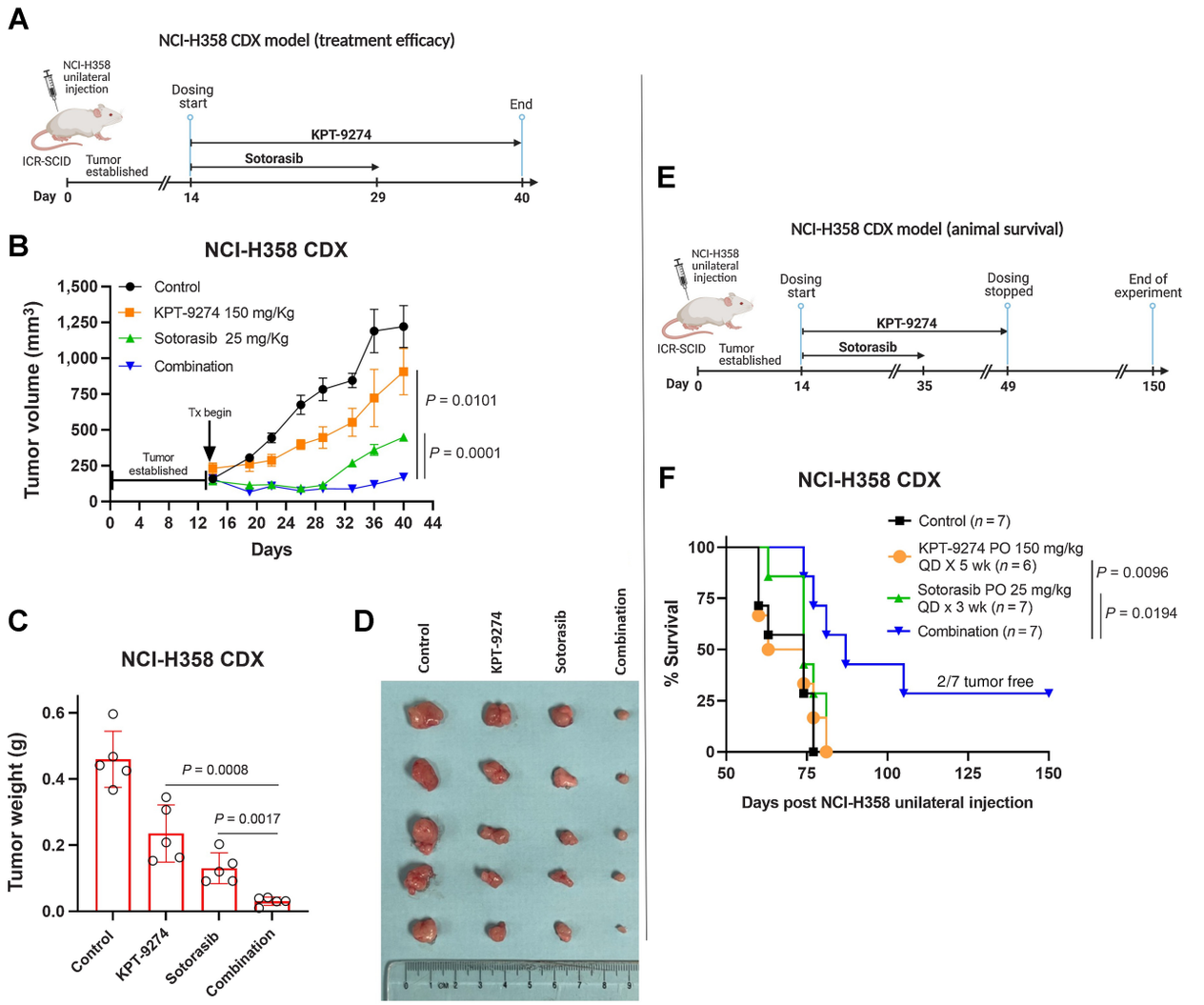

Figure 6.

Combination/maintenance therapy of KPT9274 with sotorasib induces durable tumor growth inhibition and enhances survival in a *KRAS*^{G12C}-mutant NSCLC CDX model. **A,** ICR-SCID mice subcutaneously engrafted with *KRAS*^{G12C} mutant NSCLC NCI-H358 cells were orally administered sotorasib (25 mg/kg, every day × 5) for 15 days in the single agent and combination groups, while KPT9274 (150 mg/kg every day × 5) was dosed for 26 days in both the groups. This study timeline has been created with BioRender.com (License#*DK259JM3LE*). Treatment of mice carrying the CDX with KPT9274 and sotorasib combination results in significant decrease in tumor volumes (**B**), tumor weights (**C**), and tumor sizes (**D**). A two-tailed unequal variance Student *t* test was performed to statistically compare tumor volumes and tumor weights at the end of experiment. **E,** In another experiment, mice unilaterally transplanted with NCI-H358 cells were administered with sotorasib (3 weeks), KPT9274 (5 weeks) or their combination daily five times a week by oral gavage. This study timeline has been created with BioRender.com (License#*HN259JLWT4*). **F,** Two mice (29% survival) in the combination treatment group survived and remained tumor free till the culmination of the study, that is, 150 days posttransplantation. Statistical comparison of survival curves was performed by log-rank (Mantel–Cox) test.

A combination therapy employing KRAS^{G12C} and PAK4 inhibitors can prove to be effective, especially considering that the KRAS^{G12Ci} monotherapy has already been reported to result in the emergence of drug resistant subpopulations of cancer cells (37–39). Because the pattern of resistance to KRAS inhibitors is usually heterogenous and resistance emerges due to more than one mechanism, we posit that a combination approach that can simultaneously target multiple nodes in the growth and survival pathways of cancer cells would be a more plausible strategy to circumvent resistance. Therefore, we hypothesized that using a PAK4i in combination with a KRAS^{G12Ci} would eliminate cancer cells that have developed resistance to the latter. This proposition was validated when we tested the PAK4i KPT9274 against sotorasib-resistant cancer cell line (MIA-AMG-R) and found that MIA-AMG-R cells were indeed sensitive to KPT9274, even more than the parental *KRAS*^{G12C}-mutant PDAC cells (MIA PaCa-2). Taken together, these results suggest that targeting PAK4 activity may serve as a viable therapeutic approach for overcoming resistance to KRAS^{G12C} inhibitors.

Inhibition of PAK4 by KPT9274 has been shown to enhance the efficacy of anti–PD-1 immunotherapy in a murine melanoma CDX model (40). In a previous study, our group demonstrated the antitumor activity of KPT9274 in xenograft models of PDAC and its ability

to overcome drug resistance and stemness (20). In another study, pharmacologic inhibition of PAK4 inhibited the growth of various human tumor cells both *in vitro* and *in vivo* (41). The administration of PF3758309, another PAK4i, significantly reduced the growth of colorectal tumors in patient-derived xenograft models of colorectal cancer (42). Similarly, in this study, we showed that administering a PAK4i in combination with a $KRAS^{G12Ci}$ resulted in extended survival and antitumor effects in $KRAS^{G12C}$-mutant CDX models.

The results of our study indicated that combining a PAK4i with a $KRAS^{G12Ci}$ can effectively suppress the growth of cancer cells carrying $KRAS^{G12C}$ mutations in both 2D and 3D cell cultures. Moreover, this combination treatment substantially reduced the clonogenic potential of $KRAS^{G12C}$-mutant cancer cells. Using $KRAS^{G12C}$-mutant tumor xenograft models, we demonstrated that the combination of KPT9274 and sotorasib was more effective at reducing tumor growth and improving survival rates. Our results also underscore the potential of KPT9274 as an adjunct for sotorasib therapy. The underlying mechanisms for the antitumor effects involve the capacity of the combination to inhibit cell growth and survival signaling, and to impede cell-cycle progression by suppressing CDK4/6 and cyclin D1 expression. It should be noted that the combination of adagrasib and CDK4/6 inhibitor palbociclib is being evaluated in patients who have shown resistance to $KRAS^{G12Ci}$ alone (KRYSTAL-16). The results of this trial show that the combination can be administered safely with manageable toxicity and some signs of initial efficacy are being observed.

Our *in vivo* findings corroborate the *in vitro* results that KPT9274 treatment can sensitize cancer cells that have developed resistance to $KRAS^{G12Ci}$. Furthermore, these results also imply that combining KPT9274 with sotorasib (or other $KRAS^{G12C}$ inhibitors) can have synergistic effects in patients with cancer who have developed resistance to $KRAS^{G12Ci}$ therapy. To investigate this possibility, clinical studies evaluating the effectiveness of combining KPT9274 with sotorasib in patients who have not responded to sotorasib therapy are warranted. If successful, this innovative combination treatment could offer significant benefits for individuals with $KRAS^{G12C}$-mutant cancers.

Authors' Disclosures

M. Nagasaka reports personal fees from AstraZeneca, Daiichi-Sankyo, Novartis, EMD Serono, Pfizer, Lilly, Genentech, Regeneron, Caris Life Sciences, Takeda, Janssen, Mirati, Blueprint Medicine; and other support from AnHeart Therapeutics outside the submitted work. O. Alkhalili reports grants from NIH during the conduct of the study. I. Azar reports personal fees from AstraZeneca outside the submitted work. E. Baloglu reports other support from Karyopharm Therapeutics outside the submitted work; in addition, E. Baloglu has a patent for KPT-9274 issued to Karyopharm Therapeutics; and is currently a consultant for Karyopharm Therapeutics. W. Senapedis reports personal fees from Karyopharm Therapeutics and personal fees from Omega Therapeutics outside the submitted work; in addition, W. Senapedis has a patent for WO2017031213A1 issued to Karyopharm Therapeutics, a patent for WO2016100515A1 issued to Karyopharm Therapeutics, a patent for US10363247B2 issued to Karyopharm Therapeutics, and a patent for WO2017031204A1 issued to Karyopharm Therapeutics. B.F. El-Rayes reports grants from Merck, Roche, Novartis, AstraZeneca, and grants from BMS outside the submitted work. A.S. Azmi reports other support from GLG, Guidepoint; grants and other support from Karyopharm; grants from Eisai, Janssen, and grants from Rhizen outside the submitted work. No disclosures were reported by the other authors.

Authors' Contributions

H.Y. Khan: Data curation, formal analysis, investigation, visualization, methodology, writing–original draft. **M. Nagasaka:** Data curation, writing–review and editing. **A. Aboukameel:** Formal analysis, investigation, methodology. **O. Alkhalili:** Data curation, formal analysis. **M.H. Uddin:** Investigation, visualization. **S.F. Bannoura:** Validation. **Y. Mzannar:** Validation. **I. Azar:** Formal analysis. **E.W. Beal:** Resources. **M.E. Tobon:** Resources. **S.H. Kim:** Resources. **R. Beydoun:** Supervision. **E. Baloglu:** Resources. **W. Senapedis:** Resources. **B.F. El-Rayes:** Supervision. **P.A. Philip:** Supervision. **R.M. Mohammad:** Resources, writing–review and editing. **A.F. Shields:** Supervision. **M.N. Al Hallak:** Resources, project administration. **A.S. Azmi:** Conceptualization, supervision, funding acquisition, project administration, writing–review and editing.

Acknowledgments

Work in the lab of A.S. Azmi is supported by NIH R37 grant R37CA215427 and NIH R01 grant R01CA240607. The authors thank the SKY Foundation, and UCAN CER-VIVE Foundation.

The publication costs of this article were defrayed in part by the payment of publication fees. Therefore, and solely to indicate this fact, this article is hereby marked "advertisement" in accordance with 18 USC section 1734.

Note

Supplementary data for this article are available at Molecular Cancer Therapeutics Online (http://mct.aacrjournals.org/).

Received April 25, 2023; revised July 30, 2023; accepted September 7, 2023; published first September 13, 2023.

References

1. Rodenhuis S. Ras and human tumors. Semin Cancer Biol 1992;3:241–7.
2. Canon J, Rex K, Saiki AY, Mohr C, Cooke K, Bagal D, et al. The clinical KRAS (G12C) inhibitor AMG 510 drives anti-tumour immunity. Nature 2019;575:217–23.
3. Hallin J, Engstrom LD, Hargis L, Calinisan A, Aranda R, Briere DM, et al. The KRAS G12C inhibitor MRTX849 provides insight toward therapeutic susceptibility of KRAS-mutant cancers in mouse models and patients. Cancer Discov 2020;10:54–71.
4. Ostrem JM, Peters U, Sos ML, Wells JA, Shokat KM. K-Ras(G12C) inhibitors allosterically control GTP affinity and effector interactions. Nature 2013;503:548–51.
5. Skoulidis F, Li BT, Dy GK, Price TJ, Falchook GS, Wolf J, et al. Sotorasib for lung cancers with *KRAS* p.G12C mutation. N Engl J Med 2021;384:2371–81.
6. Jänne PA, Riely GJ, Gadgeel SM, Heist RS, Ou SI, Pacheco JM, et al. Adagrasib in non-small-cell lung cancer harboring a *KRASG12C* mutation. N Engl J Med 2022;387:120–31.
7. Blair HA. Sotorasib: first approval. Drugs 2021;81:1573–9. Erratum in: Drugs. 2021;81:1947.
8. Dhillon S. Adagrasib: first approval. Drugs 2023;83:275–85.
9. Won SY, Park JJ, Shin EY, Kim EG. PAK4 signaling in health and disease: defining the PAK4-CREB axis. Exp Mol Med 2019;51:1–9.
10. Tabusa H, Brooks T, Massey AJ. Knockdown of PAK4 or PAK1 inhibits the proliferation of mutant KRAS colon cancer cells independently of RAF/MEK/ERK and PI3K/AKT signaling. Mol Cancer Res 2013;11:109–21.
11. Cai S, Ye Z, Wang X, Pan Y, Weng Y, Lao S, et al. Overexpression of P21-activated kinase 4 is associated with poor prognosis in non-small cell lung cancer and promotes migration and invasion. J Exp Clin Cancer Res 2015;34:48.
12. Park MH, Lee HS, Lee CS, You ST, Kim DJ, Park BH, et al. p21-Activated kinase 4 promotes prostate cancer progression through CREB. Oncogene 2013;32:2475–82.
13. Ahn HK, Jang J, Lee J, Se Hoon P, Park JO, Park YS, et al. P21-activated kinase 4 overexpression in metastatic gastric cancer patients. Transl Oncol 2011;4:345–9.
14. Wong LE, Chen N, Karantza V, Minden A. The Pak4 protein kinase is required for oncogenic transformation of MDA-MB-231 breast cancer cells. Oncogenesis 2013;2:e50.
15. Chen S, Auletta T, Dovirak O, Hutter C, Kuntz K, El-ftesi S, et al. Copy number alterations in pancreatic cancer identify recurrent PAK4 amplification. Cancer Biol Ther 2008;7:1793–802.

16. Davis SJ, Sheppard KE, Pearson RB, Campbell IG, Gorringe KL, Simpson KJ. Functional analysis of genes in regions commonly amplified in high-grade serous and endometrioid ovarian cancer. Clin Cancer Res 2013;19:1411–21.
17. Begum A, Imoto I, Kozaki K, Tsuda H, Suzuki E, Amagasa T, et al. Identification of PAK4 as a putative target gene for amplification within 19q13.12-q13.2 in oral squamous-cell carcinoma. Cancer Sci 2009;100:1908–16.
18. Park JJ, Park MH, Oh EH, Soung NK, Lee SJ, Jung JK, et al. The p21-activated kinase 4-Slug transcription factor axis promotes epithelial-mesenchymal transition and worsens prognosis in prostate cancer. Oncogene 2018;37:5147–59.
19. Qu J, Cammarano MS, Shi Q, Ha KC, de Lanerolle P, Minden A. Activated PAK4 regulates cell adhesion and anchorage-independent growth. Mol Cell Biol 2001;21:3523–33.
20. Aboukameel A, Muqbil I, Senapedis W, Baloglu E, Landesman Y, Shacham S, et al. Novel p21-activated kinase 4 (PAK4) allosteric modulators overcome drug resistance and stemness in pancreatic ductal adenocarcinoma. Mol Cancer Ther 2017;16:76–87.
21. Chan CH, Chiou LW, Lee TY, Liu YR, Hsieh TH, Yang CY, et al. PAK and PI3K pathway activation confers resistance to KRAS^{G12C} inhibitor sotorasib. Br J Cancer 2023;128:148–59.
22. Fu X, Feng J, Zeng D, Ding Y, Yu C, Yang B. PAK4 confers cisplatin resistance in gastric cancer cells via PI3K/Akt- and MEK/ERK-dependent pathways. Biosci Rep 2014;34:e00094.
23. Shu XR, Wu J, Sun H, Chi LQ, Wang JH. PAK4 confers the malignance of cervical cancers and contributes to the cisplatin-resistance in cervical cancer cells via PI3K/AKT pathway. Diagn Pathol 2015;10:177.
24. Dasgupta A, Sierra L, Tsang SV, Kurenbekova L, Patel T, Rajapakse K, et al. Targeting PAK4 inhibits ras-mediated signaling and multiple oncogenic pathways in high-risk rhabdomyosarcoma. Cancer Res 2021;81:199–212.
25. Lanman BA, Allen JR, Allen JG, Amegadzie AK, Ashton KS, Booker SK, et al. Discovery of a covalent inhibitor of KRAS^{G12C} (AMG 510) for the treatment of solid tumors. J Med Chem 2020;63:52–65.
26. Chen CY, Lu Z, Scattolin T, Chen C, Gan Y, McLaughlin M. Synthesis of *Adagrasib* (MRTX849), a covalent KRAS^{G12C} inhibitor drug for the treatment of cancer. Org Lett 2023;25:944–9.
27. Baloglu E, Golan G, Kalid O, Landesman Y, Mccauley D, Senapedis W, inventors; Karyopharm Therapeutics, assignee. Substituted benzofuranyl and benzoxazolyl compounds and uses thereof. US Patent US20160368904A1. 2018 Dec 13.
28. Khan HY, Mpilla GB, Sexton R, Viswanadha S, Penmetsa KV, Aboukameel A, et al. Calcium release-activated calcium (CRAC) channel inhibition suppresses pancreatic ductal adenocarcinoma cell proliferation and patient-derived tumor growth. cancers (Basel) 2020;12:750.
29. Khan HY, Nagasaka M, Li Y, Aboukameel A, Uddin MH, Sexton R, et al. Inhibitor of the nuclear transport protein XPO1 enhances the anticancer efficacy of KRAS G12C inhibitors in preclinical models of KRAS G12C-mutant cancers. Cancer Res Commun 2022;2:342–52.
30. Benstead-Hume G, Chen X, Hopkins SR, Lane KA, Downs JA, Pearl FMG. Predicting synthetic lethal interactions using conserved patterns in protein interaction networks. PLoS Comput Biol 2019;15:e1006888.
31. Janes MR, Zhang J, Li LS, Hansen R, Peters U, Guo X, et al. Targeting KRAS mutant cancers with a covalent G12C-specific inhibitor. Cell 2018;172:578–89.
32. Jeong WJ, Ro EJ, Choi KY. Interaction between Wnt/β-catenin and RAS-ERK pathways and an anti-cancer strategy via degradations of β-catenin and RAS by targeting the Wnt/β-catenin pathway. NPJ Precis Oncol 2018;2:5.
33. Peterson RT, Schreiber SL. Translation control: connecting mitogens and the ribosome. Curr Biol 1998;8:R248–50.
34. Yeo D, He H, Baldwin GS, Nikfarjam M. The role of p21-activated kinases in pancreatic cancer. Pancreas 2015;44:363–9.
35. Salmón M, Álvarez-Díaz R, Fustero-Torre C, Brehey O, Lechuga CG, Sanclemente M, et al. Kras oncogene ablation prevents resistance in advanced lung adenocarcinoma. J Clin Invest 2023;133:e164413.
36. Muzumdar MD, Chen PY, Dorans KJ, Chung KM, Bhutkar A, Hong E, et al. Survival of pancreatic cancer cells lacking KRAS function. Nat Commun 2017;8:1090.
37. Adachi Y, Ito K, Hayashi Y, Kimura R, Tan TZ, Yamaguchi R, et al. Epithelial-to-mesenchymal transition is a cause of both intrinsic and acquired resistance to KRAS G12C inhibitor in KRAS G12C-mutant non-small cell lung cancer. Clin Cancer Res 2020;26:5962–73.
38. Tanaka N, Lin JJ, Li C, Ryan MB, Zhang J, Kiedrowski LA, et al. Clinical acquired resistance to KRASG12C inhibition through a novel KRAS switch-II pocket mutation and polyclonal alterations converging on RAS-MAPK reactivation. Cancer Discov 2021;11:1913–22.
39. Awad MM, Liu S, Rybkin II, Arbour KC, Dilly J, Zhu VW, et al. Acquired resistance to KRASG12C inhibition in cancer. N Engl J Med 2021;384:2382–93.
40. Abril-Rodriguez G, Torrejon DY, Liu W, Zaretsky JM, Nowicki TS, Tsoi J, et al. PAK4 inhibition improves PD-1 blockade immunotherapy. Nat Cancer 2020;1:46–58.
41. Murray BW, Guo C, Piraino J, Westwick JK, Zhang C, Lamerdin J, et al. Small-molecule p21-activated kinase inhibitor PF-3758309 is a potent inhibitor of oncogenic signaling and tumor growth. Proc Natl Acad Sci U S A 2010;107:9446–51.
42. Huang C, Du R, Jia X, Liu K, Qiao Y, Wu Q, et al. CDK15 promotes colorectal cancer progression via phosphorylating PAK4 and regulating β-catenin/MEK-ERK signaling pathway. Cell Death Differ 2022;29:14–27.